

PFC/JA-84-30

Sawtooth Oscillations in the Visible  
Continuum on Alcator C

M. E. Foord and E. S. Marmor

Plasma Fusion Center  
Massachusetts Institute of Technology  
Cambridge, MA 02139

August 1984

This work was supported by the U.S. Department of Energy Contract No. DE-AC02-78ET51013. Reproduction, translation, publication, use and disposal, in whole or in part by or for the United States government is permitted.

By acceptance of this article, the publisher and/or recipient acknowledges the U.S. Government's right to retain a non-exclusive, royalty-free license in and to any copyright covering this paper.

# SAWTOOTH OSCILLATIONS IN THE VISIBLE CONTINUUM ON ALCATOR C

M. E. Foord, E. S. Marmor, MIT Plasma Fusion Center,  
Cambridge, MA 02139, USA

## ABSTRACT

The visible continuum near  $\lambda = 5360\text{\AA}$  is monitored during sawtooth discharges on the Alcator C tokamak. Because of the typically flat continuum emission profiles, effects of internal disruptions on the central continuum brightness are small. However, by averaging over many internal sawtooth periods from similar discharges, sawtooth oscillations on the continuum brightness are observed. The continuum sawteeth obtained closely resemble soft x-ray sawteeth in both phase and structure. The relative change in the central chord brightness ( $\Delta B/B$ ) due to the internal disruption is  $|\Delta B/B| \approx 0.5\%$ , which is found to be consistent with the predictions of a simple sawtooth model.

## INTRODUCTION

In this paper, we report the effects of internal disruptions on visible continuum emission from hot ( $T_e \approx 1.5 \text{ keV}$ ), dense ( $\bar{n}_e \approx 2 \times 10^{14} \text{ cm}^{-3}$ ) Alcator C plasmas. Internal disruptions (sawteeth) in tokamak plasmas were first observed in 1974 by Von Goeler et al. [1] utilizing soft x-ray measurements. Soft x-ray sawtooth oscillations are also observed on Alcator C (see Fig. 1) during low  $q_2$  ( $q_2 \equiv 5a^2 B_T / R I_p \lesssim 5$ ) discharges and are typically characterized by: 1) a sawtooth rise time in the

range of 2 to 5 ms with a disruption time of about 100  $\mu$ s; 2) a superimposed  $m = 1$  oscillation preceding the disruption; 3) inverted sawteeth from chords outside the  $q = 1$  radius. One major effect of the internal disruption is to flatten the density and temperature profiles approximately out to a mixing radius  $r_m \approx \sqrt{2}r_s$  [2], where  $r_s < r_m < a$ , and  $r_s$  is the  $q = 1$  radius.

Continuum radiation results from these plasmas when a free electron makes a transition either to a lower free energy state (bremsstrahlung) or to a bound state (recombination) in the presence of a coulomb potential. The continuum brightness is measured in the wavelength region near  $\lambda = 5360 \text{ \AA}$ , which is found to contain relatively few lines [3] and, for typically hot Alcator C discharges ( $T_e \gg 50 \text{ eV}$ ), is dominated at these low photon energies by bremsstrahlung emission. Traces of the visible continuum brightness, density, current, and central soft x-ray brightness are shown in Fig 2. Thus, the central-chord continuum brightness is equal to the line-integral bremsstrahlung emissivity and is written as:

$$1) \quad B = C_0 \int_{-a}^a \frac{n_e^2(r) Z_{\text{eff}}(r)}{T_e^{1/2}(r)} \bar{g}_{\text{ff}}(T_e(r)) \exp(-hc/\lambda T_e(r)) \, dr$$

photons/cm<sup>2</sup> sec ster A

where  $C_0 = .95 \times 10^{-13}/(\lambda 4\pi)$ ,  $\lambda = 5360 \text{ \AA}$ ,  $Z_{\text{eff}} \equiv \sum n_1 Z_1^2 / \sum n_1 Z_1$ ,  $a$  is the plasma minor radius (usually 16.5 cm),  $\bar{g}_{\text{ff}}$  is the maxwellian averaged free-free Gaunt factor,  $n_e$  is the electron density in cm<sup>-3</sup> and  $T_e$  is the electron temperature in eV. During the high density ( $\bar{n}_e \approx 2 \times 10^{14} \text{ cm}^{-3}$ ) steady state portion of the discharge,  $Z_{\text{eff}}(r)$  is approximately constant ( $\approx 1.2$ ) [3] and will be assumed constant for this analysis. Since the

Gaunt factor [4] and  $\exp(-hc/\lambda T_e)$  vary only slowly with  $T_e$  in this wavelength and temperature region, the dominant terms which vary with  $r$  in Equation 1 are  $n_e^2$  and  $T_e^{-1/2}$ .

Alcator C typically has flat density profiles ( $n_e(r) \approx n_0(1 - r^2/a^2)^\alpha$ ,  $0.5 \lesssim \alpha \lesssim 1.0$ ) and peaked temperature profiles ( $T_e(r) \approx T_0(1 - r^2/a^2)^\gamma$ ,  $1.5 \lesssim \gamma \lesssim 2.5$ ), so the continuum emission profile ( $\propto n_e^2 T_e^{-1/2}$ ) is expected to be approximately flat. A typical Abel inverted brightness profile is shown in Fig. 3. Thus, central perturbations of  $n_e$  and  $T_e$  due to the internal disruptions should have a small effect on the central brightness  $B$ . As will be shown, measurements of the relative change in the central-chord continuum brightness ( $\Delta B/B$ ) due to internal disruptions yield  $|\Delta B/B| \approx 0.5\%$ .

The continuum brightness profile is measured with a light detector system which is described in detail in Ref. 3. The optical system is comprised of a 30Å FWHM interference filter having a peak transmission of 67% at 5360Å, and a 40 cm focal length, 3 cm diameter lens which images the plasma onto an array of light pipes leading to 20 photomultiplier tubes. The spatial resolution of each chord is  $\approx 1.5$  cm at the center of the plasma. The signal from each PM tube is actively filtered ( $\tau_{RC} = 100 \mu s$ ) and then digitized at 5 kHz.

#### METHOD OF ANALYSIS

As shown in Fig. 2), the continuum brightness typically has a 3%-5% RMS ( $\nu \gtrsim 50$  Hz) fluctuation component. This component is mostly composed of a 360 Hz fluctuation, probably due mainly to the slight plasma motion caused by the 360 Hz ripple component in the horizontal and vertical fields, and to fluctuations due to photon statistics. Both sources of "noise"

are uncorrelated with internal disruptions and can be eliminated by the averaging techniques described as follows.

The central-chord continuum brightness of the  $j^{\text{th}}$  shot is denoted  $B_j(t)$  where  $1 < j < M$  and  $M$  is the total number of shots analyzed. The central-chord soft x-ray crash time (time of the internal disruption) of the  $i^{\text{th}}$  sawtooth crash during the  $j^{\text{th}}$  shot is denoted  $t_{ij}$ , where  $1 < i < N_j + 2$  and  $N_j + 2$  is the total number of sawtooth crashes during the  $j^{\text{th}}$  shot.  $N_j$  is then the total number of sawtooth time periods for the  $j^{\text{th}}$  shot (between times  $(t_{1j} + t_{2j})/2$  and  $(t_{N_j+1j} + t_{N_j+2j})/2$ ). A sawtooth time period is defined as beginning at  $t = (t_{1j} + t_{1+1j})/2$  and ending at  $t = (t_{i+1j} + t_{i+2j})/2$  (see Fig. 4). By averaging the continuum brightness over a sufficient number of time periods, effects of internal disruptions on the continuum brightness are determined.

A smoothed brightness  $\bar{B}_j(t)$  of the  $j^{\text{th}}$  shot is generated by first fitting a least squares second order polynomial  $p(t')$  to  $B_j(t')$  between times  $t' = t - \tau_{SMj}/2$  and  $t' = t + \tau_{SMj}/2$ .  $\tau_{SMj}$  is a smoothing time constant for shot  $j$  and is chosen  $\approx 4\tau_{STj}$  where  $\tau_{STj}$  is the average sawtooth time period (as defined above) for shot  $j$ . The sawtooth period usually varies by less than  $\approx 20\%$  during most shots.  $\bar{B}_j(t)$  is then equated to  $p(t' = t)$  and represents a smoothed ( $\sim 1/\tau_{SMj}$ ) brightness.

We now define:

$$\frac{\delta B_j(t)}{\bar{B}_j(t)} \equiv \frac{B_j(t) - \bar{B}_j(t)}{\bar{B}_j(t)}$$

which represents the relative continuum brightness of shot  $j$  which

has been effectively high pass filtered ( $\nu \gg 1/\tau_{SMj}$ ). Between times

$$t = (t_{1j} + t_{1+1j})/2 \text{ and } t = (t_{1+1j} + t_{1+2j})/2,$$

the  $B_j(t)/\bar{B}_j(t)$  are summed into a 21 bin array by first assigning  $B_j(t^*)/\bar{B}_j(t^*)$  to the  $k^{\text{th}}$  bin element where:

$$t^* \equiv \left\{ (t_{1j} + t_{1+1j})/2 + (t_{1+2j} - t_{1j}) \frac{K}{42} \right\}$$

$$1 < K < 21 .$$

The first term in the braces is the beginning time of the sawtooth period while the remaining term is the incremental time, which is  $K/21$  of the sawtooth period duration. Since the data were digitized at 5Kz,  $t^*$  is set to the nearest 200  $\mu$ s. Figure 4 shows an example of assigning data to bins.

After summing over  $N_j$  and  $M$ , the total in each bin is divided by the total number of sawtooth periods added,  $T_M$  ( $T_M \equiv \sum_{j=1}^M N_j$ ).

The value in the  $K^{\text{th}}$  bin ( $1 < K < 21$ ) after  $M$  shots is thus:

$$\bar{F}_M(K) \equiv \frac{1}{T_M} \sum_{j=1}^M \sum_{i=1}^{N_j} \frac{B_j(t^*)}{\bar{B}_j(t^*)}$$

In general, the relative brightness of shot  $j$  can be written as a sum of an uncorrelated component  $U_j(t)$  and a correlated component  $C_j(t)$  such that:

$$\frac{B_j(t)}{\bar{B}_j(t)} = U_j(t) + C_j(t) .$$

The RMS value of the 21 bin array after adding M shots is:

$$f_{\text{RMS}}^{(M)} = \left[ \frac{\sum_{k=1}^{21} (f_{M(k)})^2}{21} \right]^{1/2}$$

$$= \frac{1}{T_M} \left[ \frac{\sum_{k=1}^{21} \left( \sum_{j=1}^M \sum_{i=1}^{N_j} U_j(\tau^*) + C_j(\tau^*) \right)^2}{21} \right]^{1/2}$$

For the case when  $U_j \gg C_j$  and M (the number of shots) is small,

$$f_{\text{RMS}}^{(M)} \sim \frac{U_{\text{RMS}}}{\sqrt{T_M}} \text{ where } U_{\text{RMS}} \text{ is the average RMS value of } U_j(t) \text{ after}$$

adding  $T_M$  sawteeth. Since  $U_j(t) \gg C_j(t)$ ,  $U_{\text{RMS}}$  is approximately the RMS value of  $B(t)/B(t)$ . If  $C_j(t)$  has a sawtooth-like structure (see Fig. 5) which crashes from a relative amplitude  $+C_0/2$  to  $-C_0/2$ , then for large  $T_M$ ,  $f_{\text{RMS}}^{(M)}$  should approach the RMS value of a sawtooth which is  $(0.29)|C_0|$ . Thus  $f_{\text{RMS}}^{(M)}$  should approach a constant which is proportional to the sawtooth amplitude, after averaging over a sufficient number of sawtooth periods. For the sawtooth waveform described above, this "sufficient" number is:

$$T_M \gg \left( \frac{U_{\text{RMS}}}{(0.29)C_0} \right)^2$$

For example, if  $C_0 = 0.5\%$  and  $U_{\text{RMS}} = 3\%$  then  $T_M \gg 428$ . Since each shot only has from 30 to 60 sawteeth, many shots need to be averaged together.

## EXPERIMENTAL RESULTS

Figure 6) shows the relative continuum fluctuation  $\bar{F}_M(K)$  after adding 675 923, and 1623 sawtooth periods ( $T_M$ ) in which  $\bar{U}_{RMS} \approx 3.4\%$ ,  $\bar{\tau}_{ST} \approx 5$  msec,  $\bar{q}_\ell \approx 2.7 \pm 0.2$  and  $\bar{r}_m/a \approx 0.3 \pm 0.05$  as determined from a soft x-ray array. The "-" over a variable indicates an average over all shots. The continuum fluctuation appears to converge to a sawtooth-like waveform with  $|\Delta B/B| \approx 0.5\%$ . The relative standard deviation around a "best fit" sawtooth (see Fig. 6) after adding 1623 periods is calculated to be  $\approx 0.085\%$ , which is consistent with  $3.4\%/\sqrt{1623} = 0.083\%$ . Fig. 7 shows the bin RMS  $\bar{F}_{RMS}(M)$  vs.  $T_M$  (the total number of sawteeth added). For  $T_M \gg (3.4/((.29)(.5)))^2 = 583$ , the bin RMS fluctuation approaches  $0.29|\Delta B/B| = 0.14\%$  as the "noise" is averaged out.

To study the effects of internal disruptions on edge emission, the continuum filter was replaced by a CIII filter ( $\lambda = 4651\text{\AA}$ , 12\text{\AA} FWHM). For typical Alcator C discharges ( $T_{e0} \approx 1-2$  keV) the CIII emission is localized near the limiter radius and is much brighter than the continuum integrated over the 12 \text{\AA} band pass. Thus the signal in this case is strongly dominated by CIII emission from the plasma edge.

Figure 8 shows the relative fluctuation level  $\bar{F}_M(K)$  with the CIII filter after averaging over 1172 sawtooth periods. For these data  $\bar{U}_{RMS} \approx 3.5\%$  and  $\bar{\tau}_{ST} \approx 5$  ms.  $|\Delta B/B| < 0.1\%$  which is consistent with the fact that sawteeth are a result of central perturbations ( $r < r_m$ ) in the density and temperature profiles.

## SAWTOOTH MODELLING

Since 1974, much theoretical and experimental work has been done in



modelling the internal disruption [5-8]. For the purposes of this paper, the density and temperature profiles are modelled just before and just after the internal disruption, allowing the determination of  $\Delta B/B$ . The initial density and temperature profiles used are  $n(r) = n_0(1 - r^2/a^2)^\alpha$ ,  $T(r) = T_0(1 - r^2/a^2)^\gamma$  where  $\alpha$  and  $\gamma$  are independently determined variables. These profiles are then instantaneously flattened out to radius  $r_m$ , with total energy and particles conserved (see Fig. 9). Figure 10 shows a calculation of  $\Delta B/B$  for  $r_m/a=0.3$ . Also plotted on Fig. 10 is the inferred  $|\Delta B/B| \approx 0.5\%$  (from Fig. 5) in which  $\bar{r}_m/a \approx 0.3 \pm .05$  and  $\bar{\gamma} \approx 1.8$  (calculated from  $I_p$  and  $q_0 \approx .9$ ). The inferred value of  $\Delta B/B$  is thus consistent with this simple internal disruption model, within the statistical uncertainties of the sampled data and shot to shot variations in density and temperature profiles.

#### CONCLUSION AND DISCUSSION

Sawtooth oscillations have been observed for the first time on the visible continuum central chord brightness in a tokamak plasma. These oscillations result from a central periodic flattening of density and temperature profiles, exhibit a sawtooth-like structure and are in phase with internal disruptions as observed in soft x-ray emission. As the sawtooth instability perturbs primarily the central regions of these moderate  $q_l$ , ohmically heated tokamak plasmas, its effect on the visible continuum signal provides further proof that this emission is also coming from the core of the plasma, rather than being due primarily to edge radiation. The fact that the effect is small is a direct consequence of the offsetting density and temperature dependences of the bremsstrahlung at these photon energies. The simple model used for the internal disruption seems sufficient for predicting  $\Delta B/B$  for the observed temperature and density profiles.

Preliminary data taken during pellet fueled discharges [9], where the density can become highly peaked ( $n_e(0)/\bar{n}_e = 2 - 2.5$ ) and  $|\Delta B/B| \approx 5\%-10\%$ , have also shown good agreement with this model. In these cases, each sawtooth crash is readily observable on the central chord visible continuum brightness, without the need to average over disruptions. Further studies to follow the time evolution of the emission profiles during these large sawteeth are being pursued.

#### ACKNOWLEDGEMENTS

The authors wish to thank the entire Alcator Group, particularly R.S. Granetz and J.L. Terry for helpful discussions concerning this work, and M. J. Psaila for invaluable help in data reduction.

## REFERENCES

- [1] VON GOELER, S., STODIEK, SAUTHOFF, N., Phys. Rev. Lett., 33, 1201 (1974).
- [2] KADOMTSEV, B., Sov. J. Plasma Phys. 1, 389 (1975).
- [3] FOORD, M., MARMAR, E. S., TERRY, J. L., Rev. Sci. Instr. 53 (9), 167, Sept 1982.
- [4] KARZAS, J., LATTER, R., Astrophys. J., Suppl. Ser. 6, 1961.
- [5] DNESTROVSKII, Y., LYSENKO, S. E., SMITH, R., Sov. J. Plasma Phys., 3, 9 (1977).
- [6] JAHNS, G., SOLER, M., WADDELL, B. V., CALLEN, J. D., HICKS, H. R., Nucl. Fusion 18, (1978) 609.
- [7] VASIN, N., GORBUNOV, E. P., NEUDACHIN, S. V., PEREVERZEV, G. V., Sov. J. Plasma Phys. 8 (2), Mar 1982.
- [8] PARAIL, V., PEREVERZEV, G. V., Sov. J. Plasma Phys. 6, 1(1980).
- [9] GREENWALD, M., GWINN, D., MILORA, S., PARKER, J., et al., Phys. Rev. Lett. 53, 352 (1984).

## FIGURE CAPTIONS

- Fig. 1 Typical soft x-ray brightnesses from 8 different impact radii during a sawtooth discharge in which  $a=16.5$  cm and  $r_m \approx 8.5$  cm.
- Fig. 2 Typical traces of the central chord visible continuum brightness ( $\lambda = 5360\text{\AA}$ ), central chord soft x-ray brightness, plasma current ( $I_{\max} \approx 620$  kA), and central line-average density ( $.75 \times 10^{14}$  cm<sup>-3</sup>/fringe).
- Fig. 3 Typical Abel inverted continuum emission profile. Since the central portion of the profile is usually quite flat, the effects of sawteeth are typically small on the central chord continuum brightness. Error bars are estimated from inversions of brightness fluctuations.
- Fig. 4  $\bar{B}(t)/\bar{B}(t)$  is summed into a 21 bin array for shot  $j$ .  $t_{ij}$  is the time of the  $i$ 'th sawtooth crash for shot  $j$ . The continuum brightness (digitized at 5kHz) between  $(t_{ij} + t_{i+1j})/2$  and  $(t_{i+1j} + t_{i+2j})/2$  is summed such that the closest data point to a particular bin is added to that bin.
- Fig. 5 A sawtooth waveform with an amplitude of  $C_0$  has a RMS value of  $(.29)C_0$ . For large  $T_M$ , if  $\bar{f}_M(K)$  approaches this waveform, then  $\bar{f}_{\text{RMS}}(M)$  should approach  $(.29)|\Delta B/B|$ .
- Fig. 6  $\bar{f}_M(K)$  after adding 676, 923, and 1623 sawteeth. For  $T_M = 1623$  the RMS fluctuation of  $\bar{f}_M(K)$  around a "best fit" sawtooth (dotted line) is calculated to be 0.085%. This is consistent with the expected "noise" level after adding 1623 sawteeth with a 3.4% fluctuation level ( $3.4\%/\sqrt{1623} = 0.083\%$ ) assuming the correlated component  $C_j(t)$  is much smaller than the uncorrelated component  $U_j(t)$ . This "best fit" sawtooth has an amplitude of  $\approx 0.5\%$  which satisfies the above assumption  $((.29)(.5\%) \ll 3.4\%)$ .
- Fig. 7  $\bar{f}_{\text{RMS}}(M)$  is plotted vs.  $T_M$  (total sawteeth after shot  $M$ ). For  $T_M \gg 583$ ,  $\bar{f}_{\text{RMS}}(M)$  approaches  $(.5\%)(.29) = .14\%$  while  $\bar{U}_{\text{RMS}}/\sqrt{T_M}$  continues to decrease.

- Fig. 8  $f_M(K)$  after adding 1172 sawteeth in the case where the usual continuum filter was replaced by a CIII ( $\lambda=4651\text{\AA}$ ,  $\Delta\lambda=12\text{\AA}$ ) filter. CIII emission is localized near the limiter radius and dominates the signal integrated over this 12 $\text{\AA}$  pass band. No effects of sawteeth are observed.
- Fig. 9 Model of density and temperature profiles before (solid) and after (dotted) an internal disruption. The central temperature and density following the crash are calculated by conserving total particles and energy.
- Fig. 10 Calculations of the relative change in the central chord continuum brightness  $\Delta B/B$  utilizing the simple sawtooth model of Fig. 9.  $\Delta B/B$  is a function of the initial density and temperature profiles ( $\alpha$ ,  $\gamma$ ) and the relative mixing radius  $r_m/a$  which is 0.3 in this case. Negative values of  $\Delta B/B$  imply a sawtooth crash while positive values of  $\Delta B/B$  imply an inverted sawtooth. The "best fit" sawtooth amplitude of Fig. 6 ( $|\Delta B/B| = 0.5\% \pm .085\%$ ) is also plotted for comparison, and is seen to be consistent with the temperature and density profiles of these measurements.

Soft X-Ray  
Impact  
Radii (cm)

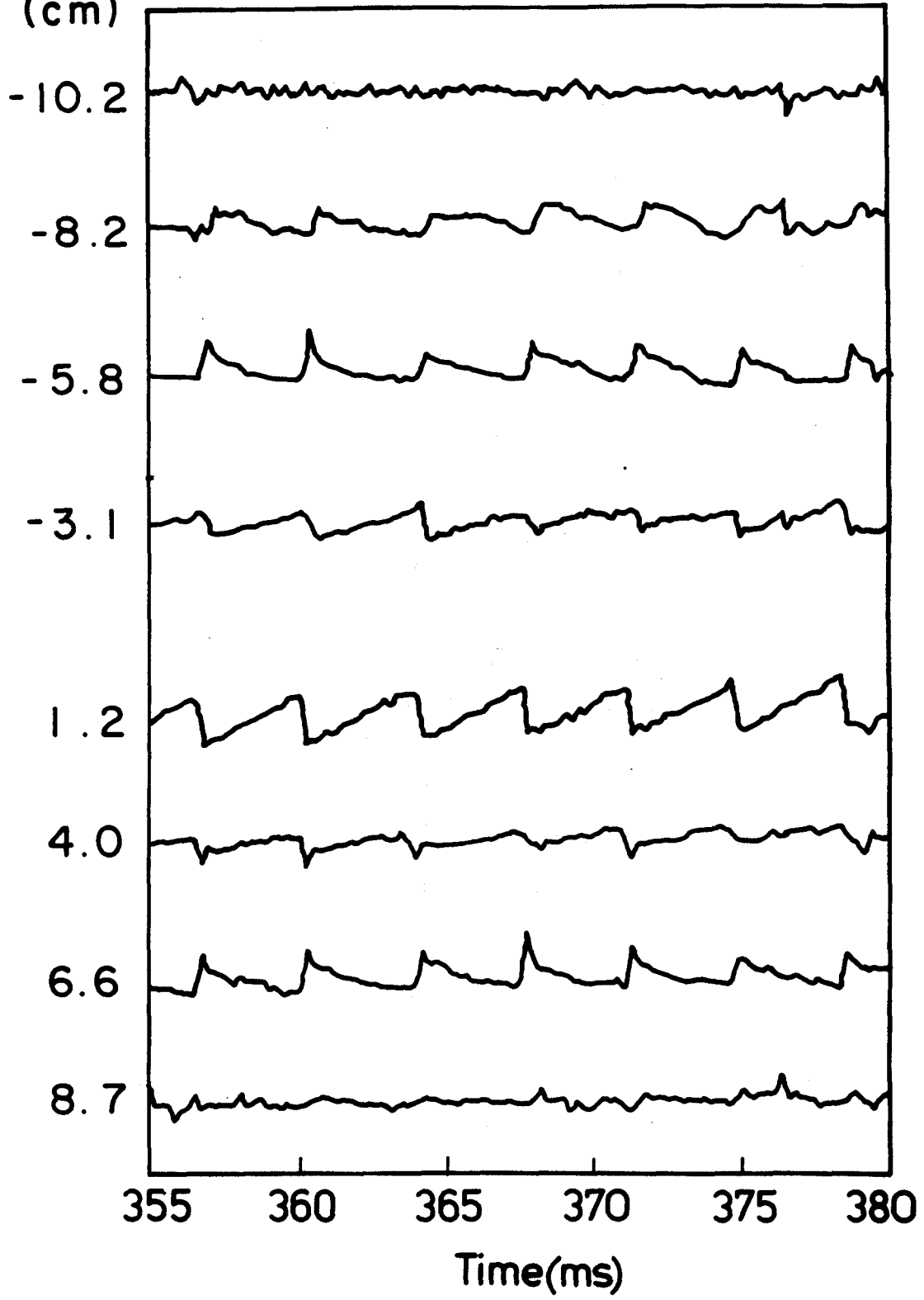


Figure 1

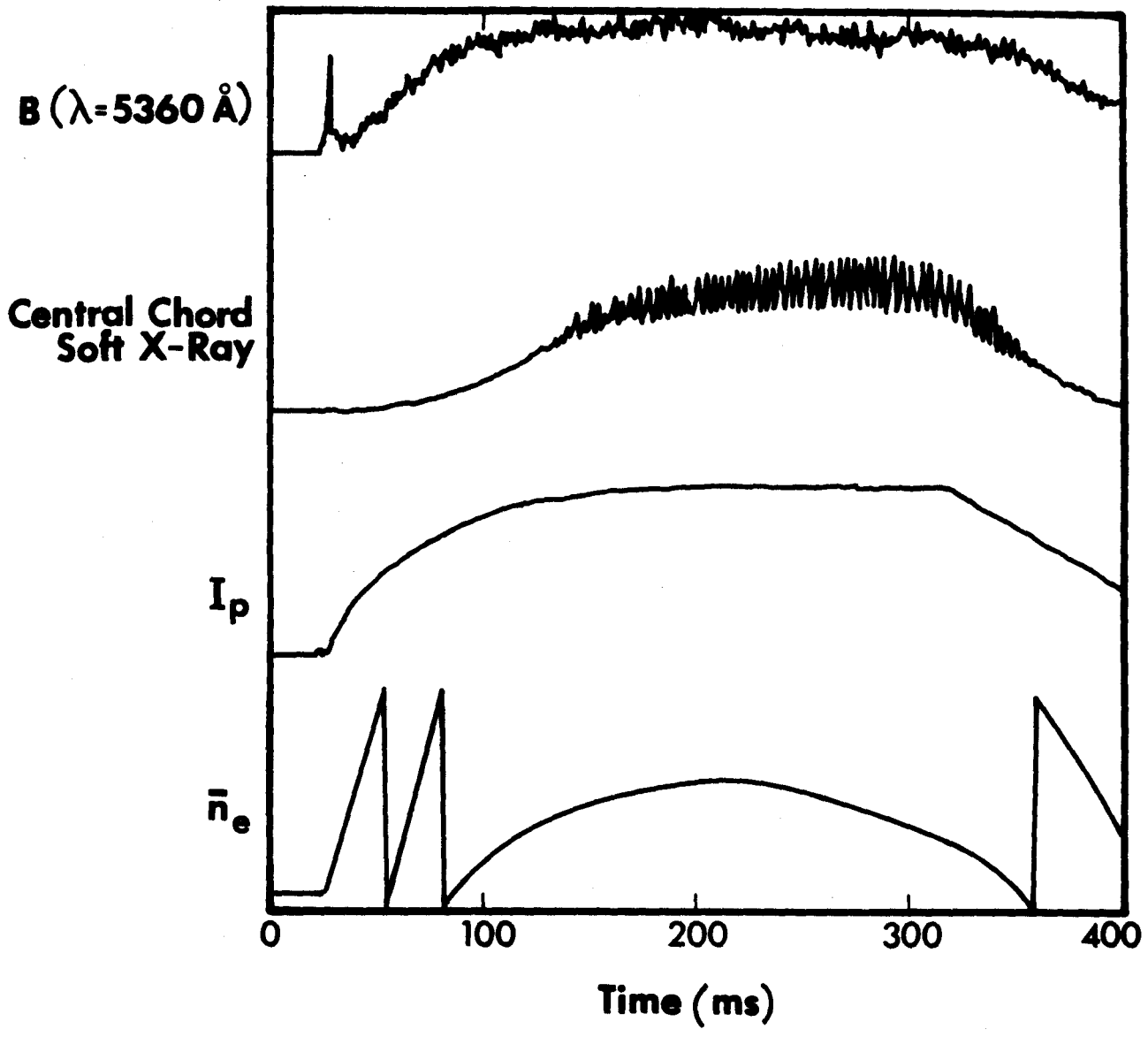


Figure 2

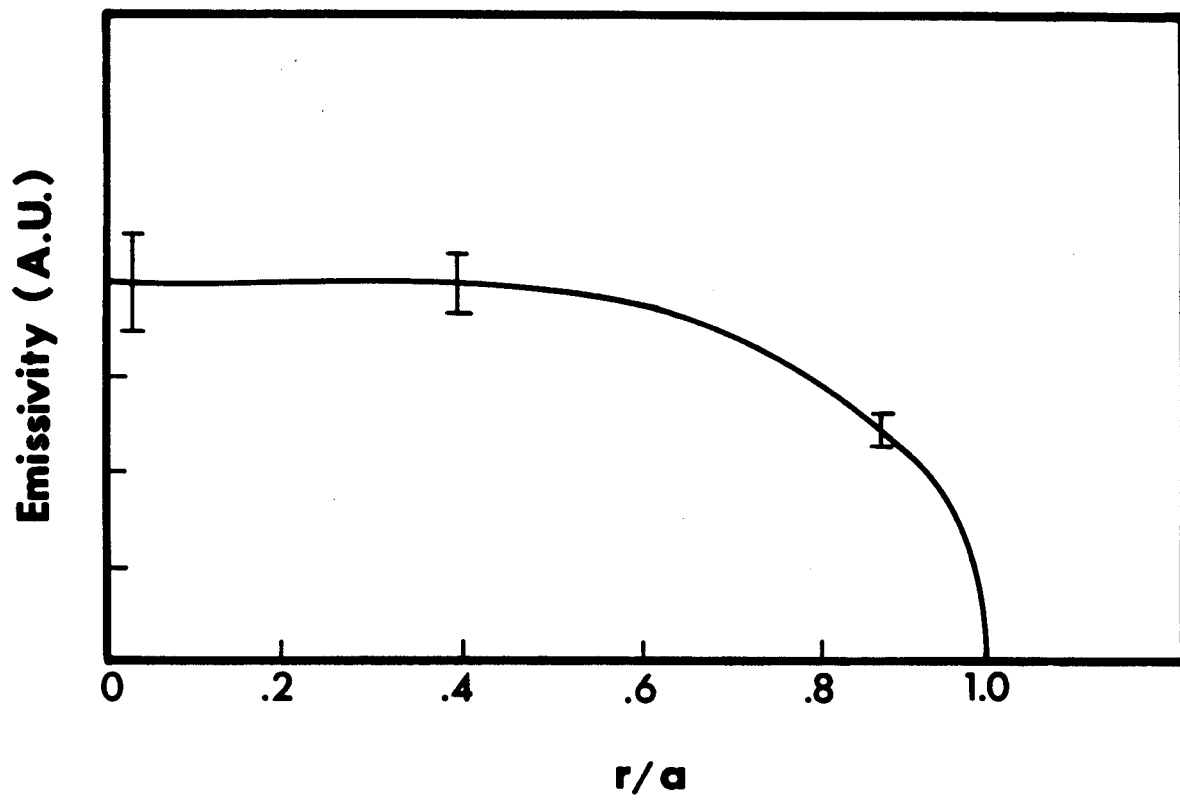


Figure 3



Central  
Soft X-Ray

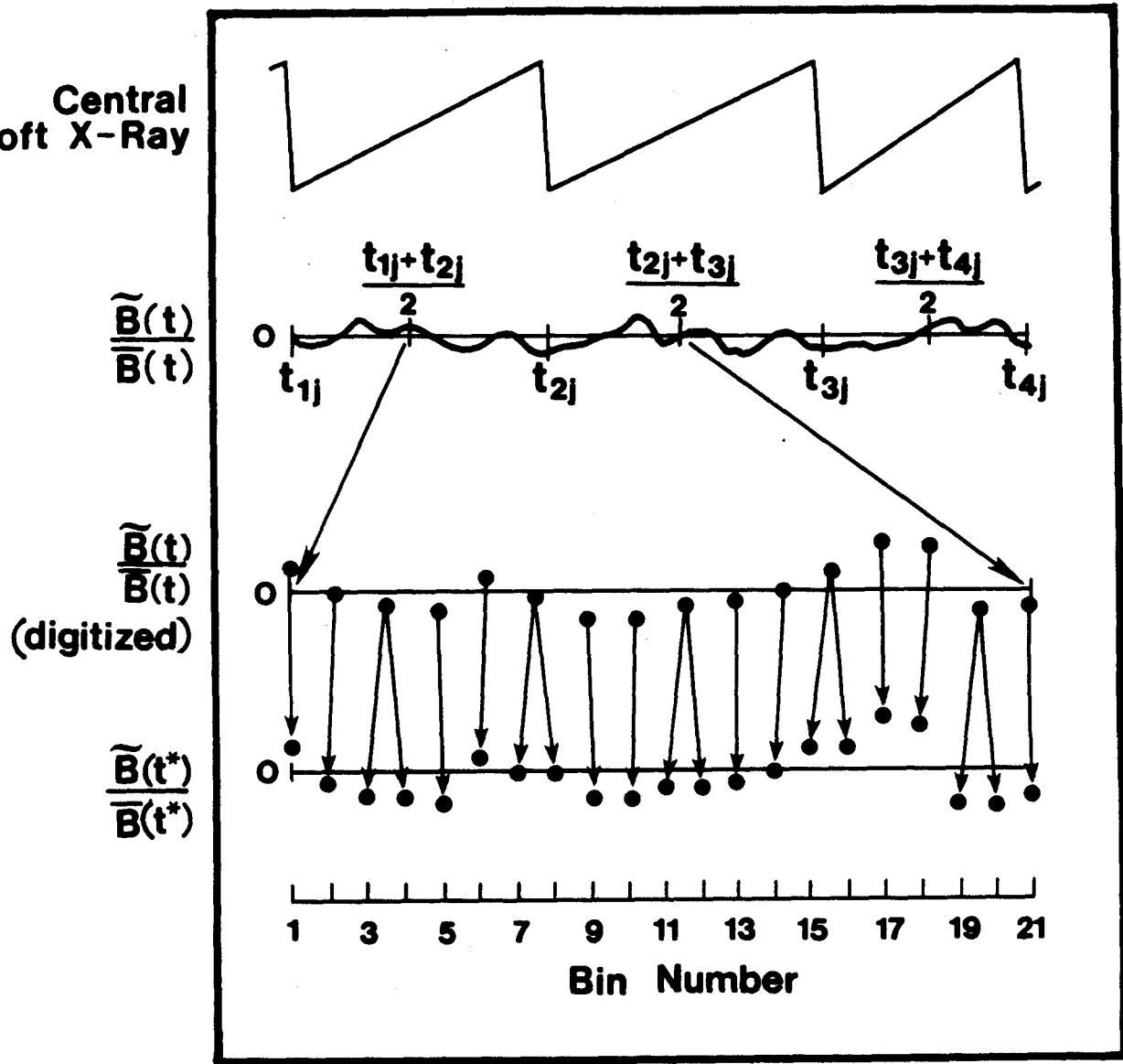


Figure 4

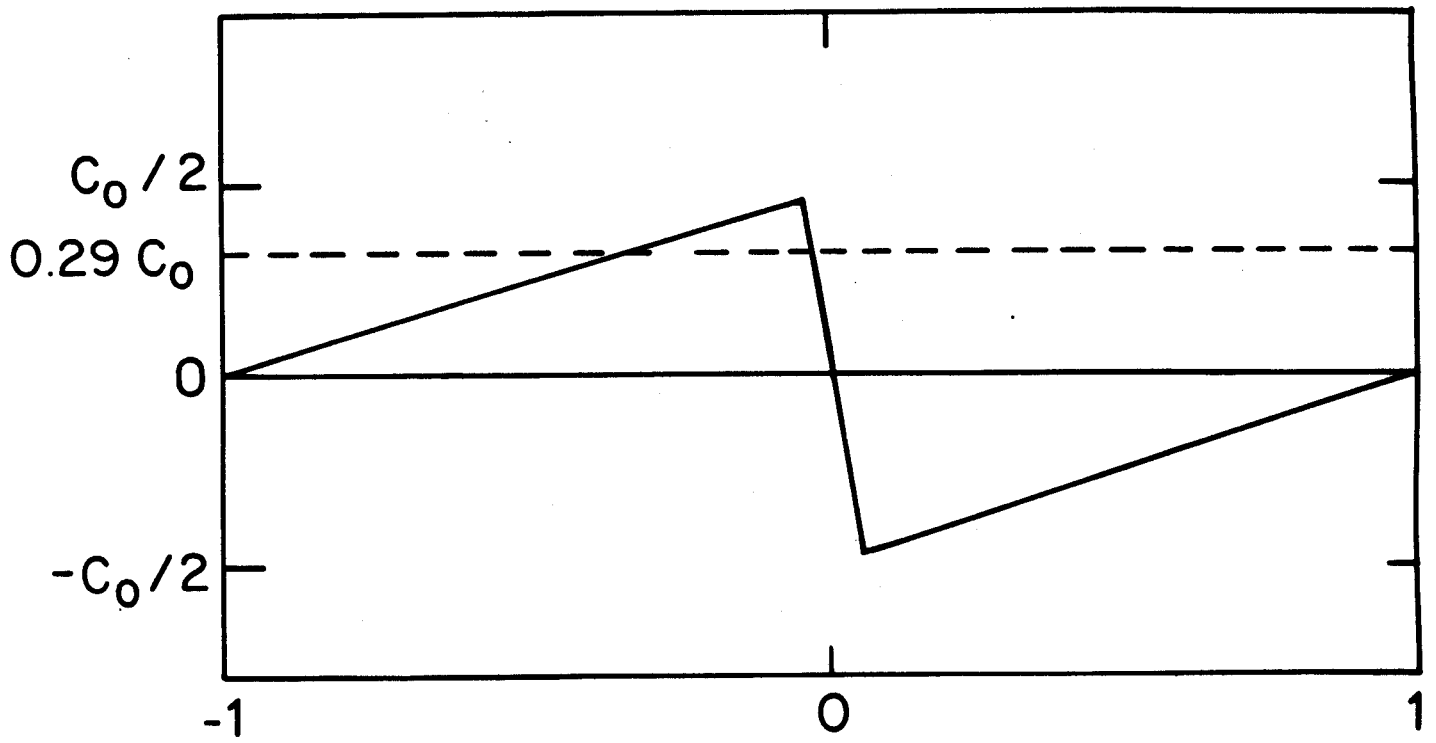


Figure 5

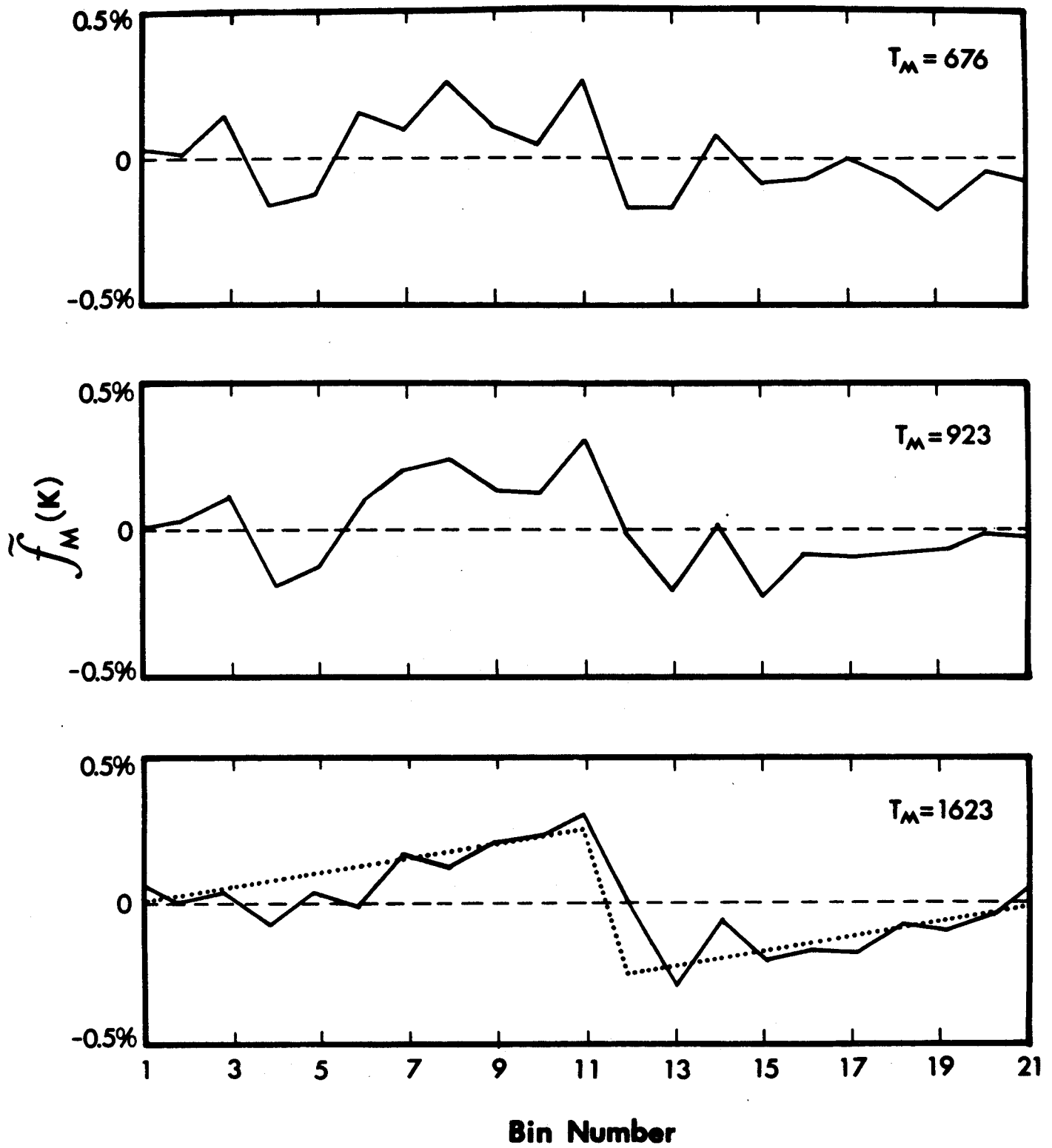


Figure 6

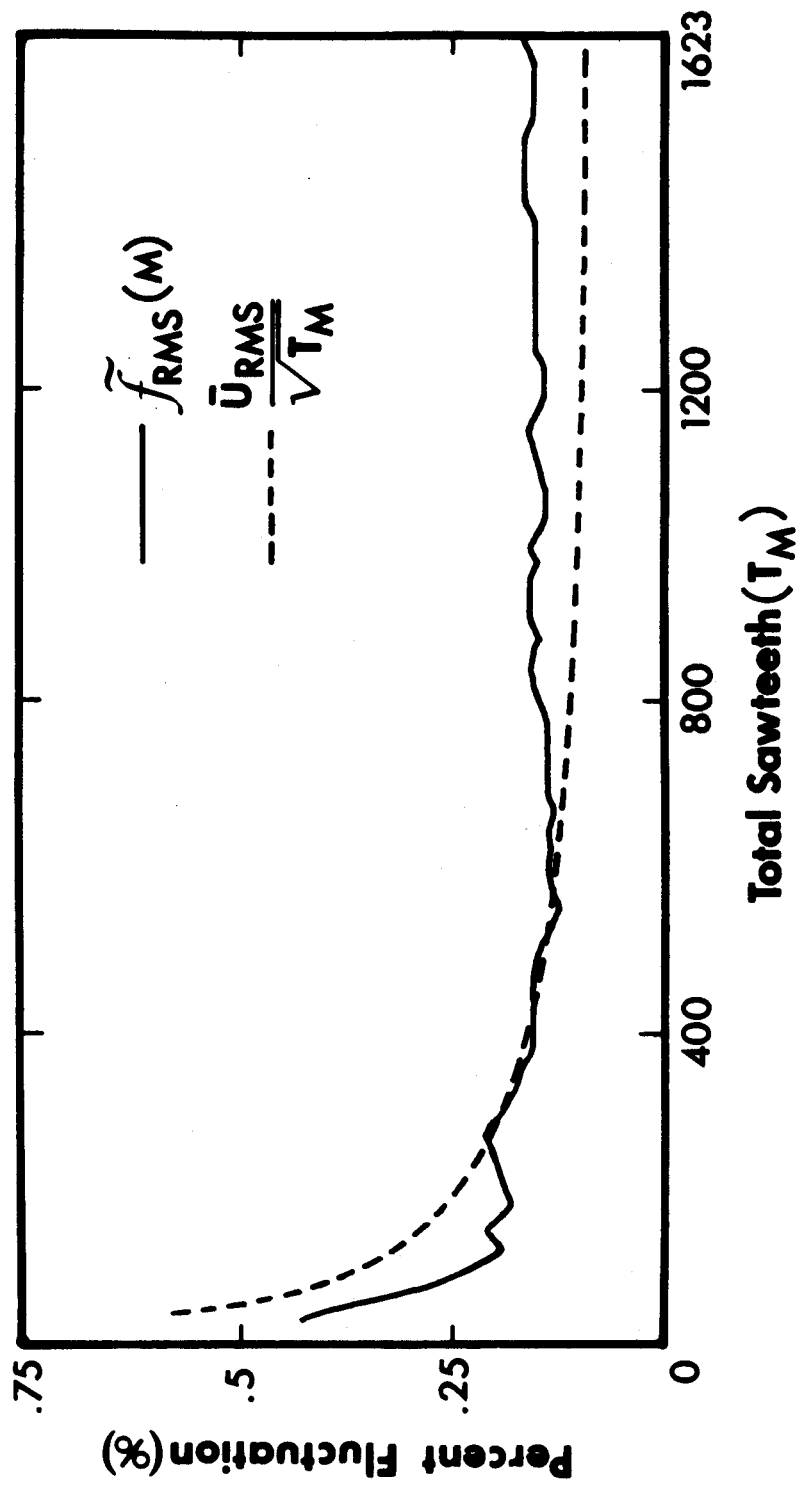


Figure 7

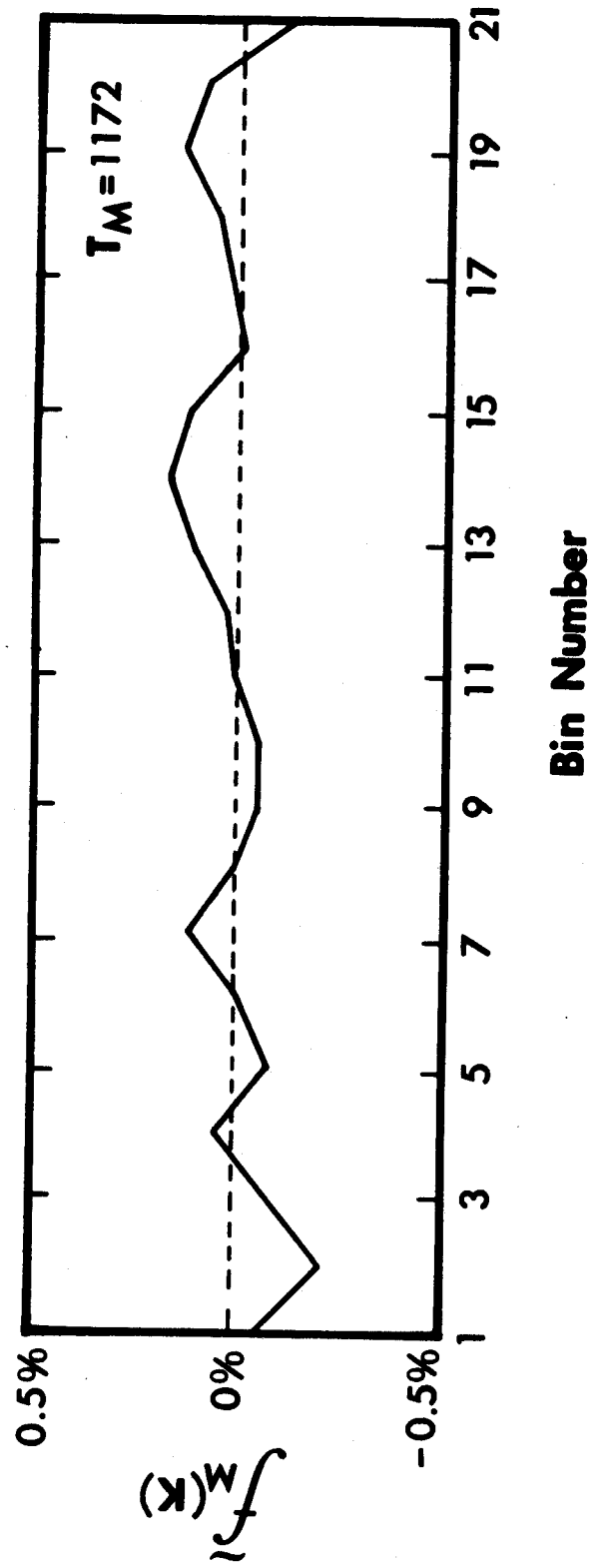


Figure 8

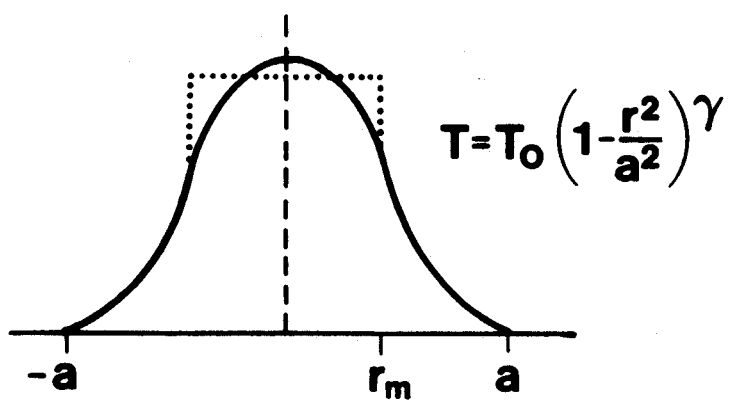
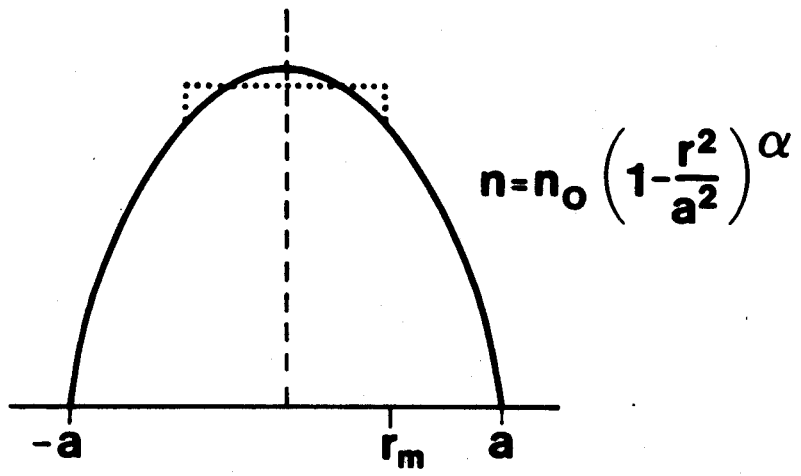


Figure 9

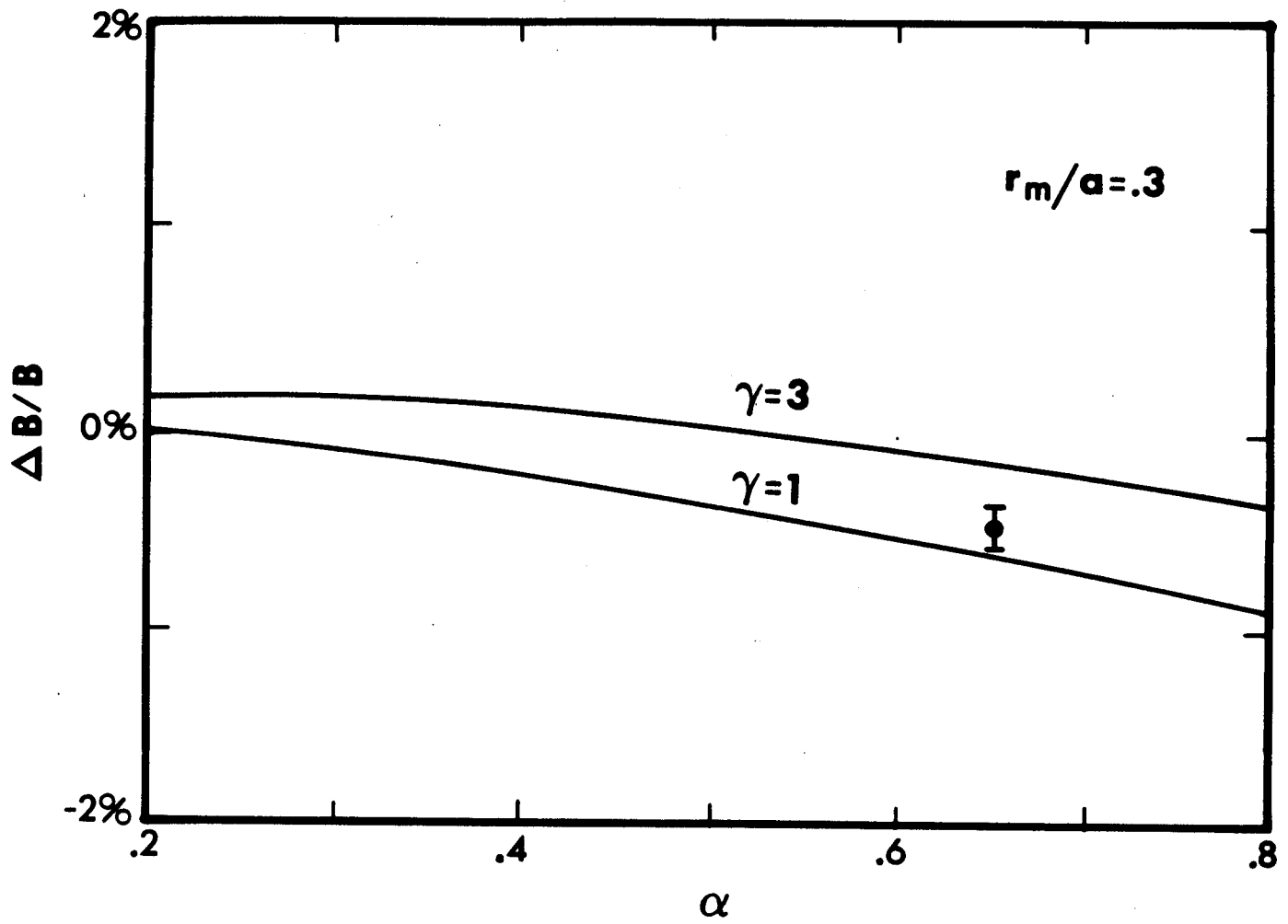


Figure 10